Large $(g-2)_\mu$ and signals of decays $e_b \to e_a\gamma$ in a $3-3-1$ model with inverse seesaw neutrinos

L. T. Hue,[1,†] H. T. Hung,[2,‡] N. T. Tham,[2,§] H. N. Long,[3,∥] and T. Phong Nguyen[4,*]

[1]*Institute for Research and Development, Duy Tan University, Da Nang City 50000, Vietnam*
[2]*Department of Physics, Hanoi Pedagogical University 2, Phuc Yen, Vinh Phuc 15000, Vietnam*
[3]*Institute of Physics, Vietnam Academy of Science and Technology, 10 Dao Tan, Ba Dinh, 10000 Hanoi, Vietnam*
[4]*Department of Physics, Can Tho University, 3/2 Street, Ninh Kieu, Can Tho City 94000, Vietnam*

(Received 8 April 2021; accepted 31 July 2021; published 31 August 2021)

We show that under current experimental bounds of the decays $e_a \to e_b\gamma$, the recent experimental data of the muon anomalous magnetic dipole moment $(g-2)_\mu$ can be explained in the framework of the $3-3-1$ model with right-handed neutrinos. In addition, all of these branching ratios can reach closely the recent experimental upper bounds.

DOI: 10.1103/PhysRevD.104.033007

I. INTRODUCTION

At present, the experimental data on the anomalous dipole magnetic moments of electron and muon $a_{e,\mu} = (g_{e,\mu}-2)/2$ show significant deviations from their values predicted by the Standard Model (SM) [1–4]. From the combination of various different contributions [2,5–23], the recent improved value of a_μ predicted by the SM is accepted widely as follows [24]: $a_\mu^{\rm SM} = 116591810(43)\times 10^{-11}$. The latest experimental measurement has been reported from Fermi National Accelerator Laboratory [25], $a_\mu^{\rm exp} = 116592061(41)\times 10^{-11}$, leading to the improved standard deviation of 4.2σ from the SM prediction, namely

$$\Delta a_\mu \equiv a_\mu^{\rm exp} - a_\mu^{\rm SM} = 251\times 10^{-11} \pm 59\times 10^{-11}. \quad (1)$$

On the other hand, the recent constraints on the charged lepton flavor violating (cLFV) decays, $e_b \to e_a\gamma$ are [26,27]:

$$\begin{aligned} &{\rm Br}(\tau\to\mu\gamma) < 4.4\times 10^{-8},\\ &{\rm Br}(\tau\to e\gamma) < 3.3\times 10^{-8},\\ &{\rm Br}(\mu\to e\gamma) < 4.2\times 10^{-13}. \end{aligned} \quad (2)$$

Many recent versions of the $3-3-1$ models were indicated that they are difficult to explain simultaneously all of these experimental constraints [28–33] with the very large TeV values of the $SU(3)_L$ symmetry scale. Namely, the discussion on Ref. [29] needs the cLFV constraints from experimental data to rule out large Δa_μ. The remaining models rule out large Δa_μ for large $SU(3)_L$ symmetry scale with order of $\mathcal{O}(1)$ TeV, if no new $SU(3)_L$ Higgs triplet or vectorlike charged lepton are added. This result can be explained qualitatively from a consequence that a one-loop contribution from a heavy gauge boson V is different from that of the $W^\pm$ boson by a small factor $m_W^2/m_V^2 \geq 10^{-3}$. Similarly, one-loop contributions from heavy Higgs boson S have a suppressed factor m_h^2/m_S^2, where m_h is the mass of the standard model (SM-like) Higgs boson. In addition, these Higgs contributions are constrained strictly by the small upper bound of ${\rm Br}(\mu\to e\gamma)$, leading to a strict constraint on the doubly Higgs mass for the $3-3-1$ models adding a $SU(3)_L$ Higgs sextet to explain the experimental neutrino oscillation data. Adding new particles as Higgs triplets or vectorlike charged leptons into the original $3-3-1$ models to generate new couplings contributing to Δa_μ is a popular way to explain successful the experimental data of a_μ [31,32], but there seems irrelevant with neutrino oscillation data. Some recent extensions of $3-3-1$ models with discrete symmetries [34,35] need a large number of new leptons and Higgs bosons for the explanation of large $\Delta a_{\mu,e}$ consistent with experiments. On the other hand, a recent note indicated that a version of the $3-3-1$ model with right-handed neutrino (331RN) with heavy neutral fermions assigned as $SU(3)_L$ gauge singlets (called the 331ISS model for short) can predict large one-loop contributions from singly charged Higgs bosons and inverse seesaw (ISS) neutrinos enough to explain the recent $(g-2)_\mu$ data [36].

*Corresponding author.
thanhphong@ctu.edu.vn
†lethohue@duytan.edu.vn
‡hthung80@gmail.com
§nguyenthitham@hpu2.edu.vn
∥hnlong@iop.vast.ac.vn

More interesting, the model contains two singly charged Higgs bosons, which may result in a special possibility that two one-loop contributions to Δa_μ are large and constructive, while those relate with cLFV decay amplitudes are strongly destructive. In this work, we will pay attention to this possibility, namely we will try to answer a question whether there exist any allowed regions of the parameter space that the destructive properties of the Higgs contributions are enough to satisfy the cLFV experimental constraints given in Eq. (2), and explain successfully the recent data given in Eq. (1). We will use the $3-3-1$ model with the general Higgs potential given in Ref. [37,38]. The $3-3-1$ models explaining active neutrino data based on the ISS mechanism has been discussed widely previously [39–42], but the interesting regions of the parameter space allowing large Δa_μ data and consistent with recent cLFV experimental constraints were not shown. In addition, the $\mathrm{Br}(\tau \to \mu\gamma, e\gamma)$ were predicted to be smaller than $\mathrm{Br}(\mu \to e\gamma)$, which is very suppressed with the recent and upcoming experimental sensitivities of the order $\mathcal{O}(10^{-9})$ [43,44]. Many other models beyond the SM with the ISS mechanism can explain consistently the experimental data of Δa_μ and cLFV constraints [45–48]. Here we analyze predictions of the $3-3-1$ model with right-handed neutrinos for the above observables.

Our work is arranged as follows. We will review the 331ISS model in Sec. II, summarize the gauge, Higgs bosons and the lepton sectors. In Sec. III, we introduce the analytic formulas to calculate the muon magnetic dipole moment and the cLFV branching ratios. In Sec. IV, we discuss on the effect of a new singly charged Higgs boson that can give one-loop contributions to Δa_μ and cLFV amplitudes enough to explain successful all the experimental data under consideration. In Sec. V, illustrations for numerical results are given to indicate the existence of the allowed regions satisfying the experimental data mentioned in this work. The conclusion is presented in the last Sec. VI, where important results will be summarized.

II. REVIEW THE 3-3-1ISS MODEL

A. Gauge bosons and fermions

The particle content of the 331ISS model was introduced in Refs. [41,49] where active neutrino masses and oscillations are originated from the ISS mechanism. The quark sector and $SU(3)_C$ representations are irrelevant in this work, and hence they are omitted here. We refer Ref. [41] for a quark discussion. The electric charge operator corresponding to the gauge group $SU(3)_L \times U(1)_X$ is $Q = T_3 - \frac{1}{\sqrt{3}}T_8 + X$, where $T_{3,8}$ are the diagonal $SU(3)_L$ generators. Each lepton family consists of a $SU(3)_L$ triplet $\psi_{aL} = (\nu_a, e_a, N_a)^T_L \sim (3, -\frac{1}{3})$ and a right-handed charged lepton $e_{aR} \sim (1,-1)$ with $a = 1,2,3$. Each left-handed neutrino $N_{aL} = (N_{aR})^c$ is equivalent with a new right-handed neutrinos defined in previous 331RN models [50]. The only difference between the two models 331RN and 331ISS is that, the 331ISS model contains three more right-handed neutrinos transforming as gauge singlets, $X_{aR} \sim (1,0)$, $a = 1,2,3$. They couple with the $SU(3)_L$ Higgs triplets to generate the neutrino mass term relating with the ISS mechanism. The three Higgs triplets $\rho = (\rho_1^+, \rho^0, \rho_2^+)^T \sim (3, \frac{2}{3})$, $\eta = (\eta_1^0, \eta^-, \eta_2^0)^T \sim (3, -\frac{1}{3})$, and $\chi = (\chi_1^0, \chi^-, \chi_2^0)^T \sim (3, -\frac{1}{3})$ have the following necessary vacuum expectation values for generating all tree-level quark masses and leptons: $\langle\rho\rangle = (0, \frac{v_1}{\sqrt{2}}, 0)^T$, $\langle\eta\rangle = (\frac{v_2}{\sqrt{2}}, 0, 0)^T$ and $\langle\chi\rangle = (0, 0, \frac{w}{\sqrt{2}})^T$.

The gauge bosons get masses through the covariant kinetic term of the Higgs triplets, $\mathcal{L}^H = \sum_{H=\chi,\eta,\rho}(D_\mu H)^\dagger (D^\mu H)$, where the covariant derivative for the electroweak symmetry is $D_\mu = \partial_\mu - igW_\mu^a T^a - ig_X T^9 X X_\mu$, $a = 1,2,\ldots,8$. Note that $T^9 \equiv \frac{I_3}{\sqrt{6}}$ and $\frac{1}{\sqrt{6}}$ for (anti)triplets and singlets [51]. Matching with the SM gives $e = g s_W$ and $\frac{g_X}{g} = \frac{3\sqrt{2}s_W}{\sqrt{3-4s_W^2}}$, where e and s_W are respective the electric charge and sine of the Weinberg angle, $s_W^2 \simeq 0.231$. The relation $\frac{g_X}{g}$ is the same for both choices of triplet or antitriplets representations of the left-handed leptons [52,53]. The derivation of this relation is summarized as follows. The $3-3-1$ models have two spontaneous breaking steps: $SU(3)_L \times U(1)_X \overset{w}{\to} SU(2)_L \times U(1)_Y \overset{v_1,v_2}{\to} U(1)_Q$. The first breaking step with $w \neq 0$ generates masses for heavy particles predicted by the $SU(3)_L$ symmetry. The neutral gauge bosons will change into the basis containing the SM ones W_μ^3 and B_μ: $(W_\mu^3, W_\mu^8, X_\mu) \overset{w\neq 0, v_1=v_2=0}{\to} (W_\mu^3, Z'_\mu, B_\mu)$. Diagonalizing the squared mass matrix of these neutral gauge bosons will get a massive eigenstate Z' with $m^2_{Z'} \sim w^2$ and two SM massless states W_μ^3 and B_μ. The relations between the two bases before and after the first breaking step are $W_\mu^8 = \frac{\beta t}{\sqrt{6+\beta^2 t^2}}B_\mu - \frac{\sqrt{6}}{\sqrt{6+\beta^2 t^2}}Z'_\mu$, and $X_\mu = \frac{\sqrt{6}}{\sqrt{6+\beta^2 t^2}}B_\mu + \frac{\beta t}{\sqrt{6+\beta^2 t^2}}Z'_\mu$, with $t \equiv g_X/g$. Inserting these relations to the covariant derivation of the $3-3-1$ gauge group and keeping the part used to identify with the SM one, we have

$$D_\mu^{3-3-1} \to D_\mu^{\mathrm{SM}} = \partial_\mu - igT^3 W_\mu^3 - i\frac{gt}{\sqrt{6+\beta^2 t^2}}(\beta T^8 + \sqrt{6}T^9 X)B_\mu,$$

which results in the consequences that g and $\frac{gt}{\sqrt{6+\beta^2 t^2}} = g t_W$ are the gauge couplings of the SM, and the $U(1)_Y$ charge of the SM is $Y/2 = \beta T^8 + \mathbb{I}X$.

Like the 331RN model, the 331ISS model includes two pairs of singly charged gauge bosons with the following physical states $W^\pm$ and $Y^\pm$ and masses

$$W_\mu^\pm = \frac{W_\mu^1 \mp iW_\mu^2}{\sqrt{2}}, \qquad Y_\mu^\pm = \frac{W_\mu^6 \pm iW_\mu^7}{\sqrt{2}},$$
$$m_W^2 = \frac{g^2}{4}(v_1^2+v_2^2), \qquad m_Y^2 = \frac{g^2}{4}(w^2+v_1^2). \tag{3}$$

The bosons $W^\pm$ are identified with the SM ones, leading to the consequence that

$$v_1^2 + v_2^2 \equiv v^2 = (246\ \text{GeV})^2. \tag{4}$$

The general Higgs potential relating with the 331RN model will be applied in our work with $v_1 \neq v_2$. We will use the following parameters for this general case.

$$t_\beta \equiv \tan\beta = \frac{v_2}{v_1}, \qquad v_1 = vc_\beta, \qquad v_2 = vs_\beta. \tag{5}$$

The parameter t_β plays a similar role known in the well-known models with two Higgs doublet and the minimal supersymmetric Standard Model. This is different from Ref. [49], where $v_1 = v_2$ was assumed so that the Higgs potential given in Ref. [54] was used to find the exact physical state of the SM-like Higgs boson. This simple condition was also used in previous discussions in $3-3-1$ models addressed with anomalous magnetic dipole moments [31,32]. As we will show below, large $t_\beta \neq 1$ is one of the key condition for predicting large $(g-2)_\mu$ consistent with experiments. The reason is that the physical states of the charged Higgs bosons are determined analytically from this Higgs potential, and only these Higgs bosons contribute significantly to one-loop corrections to the $(g-2)_\mu$.

The Yukawa Lagrangian for generating lepton masses is:

$$\mathcal{L}_l^Y = -h_{ab}^e \overline{\psi_{aL}}\rho e_{bR} + h_{ab}^\nu \epsilon^{ijk}\overline{(\psi_{aL})_i}(\psi_{bL})_j^c \rho_k^* - Y_{ab}\overline{\psi_{aL}}\chi X_{bR} - \frac{1}{2}(\mu_X)_{ba}^* \overline{(X_{aR})^c} X_{bR} + \text{H.c.}. \tag{6}$$

Here we assumed that the model under consideration respects a new lepton number symmetry $\mathcal{L}$ discussed in Ref. [38] so that the term $\overline{\psi_{aL}}\eta X_{bR}$ is not allowed in the above Yukwa Lagrangian, while the soft-breaking term $(\mu_X)_{ba}^*\overline{(X_{aR})^c}X_{bR}$ is allowed with small $(\mu_X)_{ba}$. The new lepton number $\mathcal{L}$ called by generalized lepton number [55] is defined as $L = \frac{4}{\sqrt{3}}T^8 + \mathcal{L}\mathbb{I}$, where L is the normal lepton number. The specific assignment of $\mathcal{L}$ is $\mathcal{L}(\rho) = -1/3$, $\mathcal{L}(\eta) = -2/3$, $\mathcal{L}(\chi) = 4/3$, $\mathcal{L}(\psi_{aL}) = 1/3$, which guarantees the consistence for the well-known definition of L, namely $L(\ell) = 1$ for $\ell = e_{aL,R}, \nu_{aL}$, $L(\ell) = -1$ for $\ell = N_{aL}, X_{aR}$, and $L(q) = 0$ for all SM quarks [38].

The first term in Lagrangian (6) generates charged lepton masses $m_{e_a} \equiv \frac{h_{ab}^e v_1}{\sqrt{2}}\delta_{ab}$, i.e., the mass matrix of the charged leptons is assumed to be diagonal, hence the flavor states of the charged leptons are also the physical ones. In the basis $\nu_L' = (\nu_L, N_L, (X_R)^c)^T$ and $(\nu_L')^c = ((\nu_L)^c, (N_L)^c, X_R)^T$ of the neutral leptons, Lagrangian (6) gives a neutrino mass term corresponding to a block form of the mass matrix [49], namely

$$-\mathcal{L}_{\text{mass}}^\nu = \frac{1}{2}\overline{\nu_L'}M^{\nu\dagger}(\nu_L')^c + \text{H.c.},$$
$$\text{where } M^{\nu\dagger} = \begin{pmatrix} 0 & m_D & 0 \\ m_D^T & 0 & M_R \\ 0 & M_R^T & \mu_X^\dagger \end{pmatrix}, \tag{7}$$

where M_R is a 3×3 matrix $(M_R)_{ab} \equiv Y_{ab}\frac{w}{\sqrt{2}}$, $(m_D)_{ab} \equiv \sqrt{2}h_{ab}^\nu v_1$ with $a,b = 1,2,3$. Neutrino subbases are denoted as $\nu_R = ((\nu_{1L})^c, (\nu_{2L})^c, (\nu_{3L})^c)^T$, $N_R = ((N_{1L})^c, (N_{2L})^c, (N_{3L})^c)^T$, and $X_L = ((X_{1R})^c, (X_{2R})^c, (X_{3R})^c)^T$. The mass matrix M_R does not appear in the 331RN. The Dirac neutrino mass matrix m_D must be antisymmetric. The matrix μ_X defined in Eq. (6) is symmetric and it can be diagonalized by a transformation U_X:

$$U_X^T \mu_X U_X = \text{diag}(\mu_{X,1}, \mu_{X,2}, \mu_{X,3}). \tag{8}$$

The matrix U_X will be absorbed by redefinition the states X_a, therefore μ_X will be set as the diagonal matrix given in the right hand side of Eq. (8).

The mass matrix M^ν is diagonalized by a 9×9 unitary matrix U^ν,

$$U^{\nu T}M^\nu U^\nu = \hat{M}^\nu = \text{diag}(m_{n_1}, m_{n_2}, \ldots, m_{n_9}) = \text{diag}(\hat{m}_\nu, \hat{M}_N), \tag{9}$$

where m_{n_i} $(i = 1,2,\ldots,9)$ are masses of the nine physical neutrino states n_{iL}. They consist of three active neutrinos n_{aL} $(a = 1,2,3)$ corresponding to the mass submatrix $\hat{m}_\nu = \text{diag}(m_{n_1}, m_{n_2}, m_{n_3})$, and the six extra neutrinos n_{IL} $(I = 4,5,\ldots,9)$ with $\hat{M}_N = \text{diag}(m_{n_4}, m_{n_5}, \ldots, m_{n_9})$. The ISS mechanism leads to the following approximation solution of U^ν,

$$U^\nu = \Omega\begin{pmatrix} U_{\text{PMNS}} & \mathbf{O} \\ \mathbf{O} & V \end{pmatrix},$$
$$\Omega = \exp\begin{pmatrix} \mathbf{O} & R \\ -R^\dagger & \mathbf{O} \end{pmatrix} = \begin{pmatrix} 1-\frac{1}{2}RR^\dagger & R \\ -R^\dagger & 1-\frac{1}{2}R^\dagger R \end{pmatrix} + \mathcal{O}(R^3), \tag{10}$$

where

$$R^* \simeq (-m_D^* M^{-1}, \qquad m_D^*(M_R^\dagger)^{-1}), \qquad M \equiv M_R^*\mu_X^{-1}M_R^\dagger, \tag{11}$$

$$m_D^* M^{-1} m_D^\dagger \simeq m_\nu \equiv U_{\rm PMNS}^* \hat{m}_\nu U_{\rm PMNS}^\dagger, \tag{12}$$

$$V^* \hat{M}_N V^\dagger \simeq M_N + \frac{1}{2} R^T R^* M_N + \frac{1}{2} M_N R^\dagger R, \qquad M_N \equiv \begin{pmatrix} 0 & M_R^* \\ M_R^\dagger & \mu_X \end{pmatrix}. \tag{13}$$

The relations between the flavor and mass eigenstates are

$$\nu_L' = U^\nu n_L, \quad \text{and} \quad (\nu_L')^c = U^{\nu *} (n_L)^c, \tag{14}$$

where $n_L \equiv (n_{1L}, n_{2L}, \ldots, n_{9L})^T$ and $(n_L)^c \equiv ((n_{1L})^c, (n_{2L})^c, \ldots, (n_{9L})^c)^T$. The standard form of the lepton mixing matrix $U_{\rm PMNS}$ is the function of three angles θ_{ij}, one Dirac phase δ and two Majorana phases α_1, and α_2 [56], namely

$$\begin{aligned} U_{\rm PMNS}^{\rm PDG} &= \begin{pmatrix} 1 & 0 & 0 \\ 0 & c_{23} & s_{23} \\ 0 & -s_{23} & c_{23} \end{pmatrix} \begin{pmatrix} c_{13} & 0 & s_{13} e^{-i\delta} \\ 0 & 1 & 0 \\ -s_{13} e^{i\delta} & 0 & c_{13} \end{pmatrix} \begin{pmatrix} c_{12} & s_{12} & 0 \\ -s_{12} & c_{12} & 0 \\ 0 & 0 & 1 \end{pmatrix} \text{diag}(1, e^{i\alpha_1}, e^{i\alpha_2}) \\ &= U_{\rm PMNS}^0 \text{diag}(1, e^{i\alpha_1}, e^{i\alpha_2}), \end{aligned} \tag{15}$$

where $s_{ij} \equiv \sin\theta_{ij}$, $c_{ij} \equiv \cos\theta_{ij} = \sqrt{1 - s_{ij}^2}$, $i, j = 1, 2, 3$ $(i < j)$, $0 \le \theta_{ij} < 90$ [Deg.] and $0 < \delta \le 720$ [Deg.]. The Majorana phases are chosen in the range $-180 \le \alpha_i \le 180$ [Deg.]

In this paper, we will work on the normal ordered scheme (NO) of the active neutrino masses, which allows $\delta = \pi$ using in this work. The respective best fit and the confidence level of 3σ of the neutrino oscillation experimental data is given as [4]

$$\begin{aligned} s_{12}^2 &= 0.32, 0.273 \le s_{12}^2 \le 0.379; \\ s_{23}^2 &= 0.547, 0.445 \le s_{23}^2 \le 0.599; \\ s_{13}^2 &= 0.0216, 0.0196 \le s_{13}^2 \le 0.0241; \\ \delta &= 218[\text{Deg}], 157\ [\text{Deg}] \le \delta \le 349\ [\text{Deg}]; \\ \Delta m_{21}^2 &= 7.55 \times 10^{-5}[\text{eV}^2], \qquad 7.05 \times 10^{-5}[\text{eV}^2] \le \Delta m_{21}^2 \le 8.24 \times 10^{-5}[\text{eV}^2]; \\ \Delta m_{32}^2 &= 2.424 \times 10^{-3}[\text{eV}^2], \qquad 2.334 \times 10^{-3}[\text{eV}^2] \le \Delta m_{32}^2 \le 2.524 \times 10^{-3}[\text{eV}^2]. \end{aligned} \tag{16}$$

The above CP phase is consistent with the updated one given in Ref. [57], where the allowed range corresponding to 3σ confidence level are $-3.41 \le \delta \le -0.03$ $(164.6 \le \delta \le 358.3$ [Deg.]) for the NO scheme. The lepton mixing matrix defined in Eq. (12) relates with the experimental parameters appearing in Eq. (16) are [56]

$$s_{12}^2 = \frac{|(U_{\rm PMNS})_{12}|^2}{1 - |(U_{\rm PMNS})_{13}|^2}, \qquad s_{13}^2 = |(U_{\rm PMNS})_{13}|^2, \qquad s_{23}^2 = \frac{|(U_{\rm PMNS})_{23}|^2}{1 - |(U_{\rm PMNS})_{13}|^2}. \tag{17}$$

Additionally, it is easily to derive that

$$\begin{aligned} e^{i\delta} &= \frac{c_{23}(c_{12}^2 + y s_{12}^2)}{s_{13} s_{23} s_{12} c_{12} (1 - y)}, \qquad y = \frac{(U_{\rm PMNS})_{22}(U_{\rm PMNS})_{11}}{(U_{\rm PMNS})_{12}(U_{\rm PMNS})_{21}}, \\ e^{i\alpha_1} &= \frac{(U_{\rm PMNS})_{12} c_{12}}{|(U_{\rm PMNS})_{11}| s_{12}}, \qquad e^{i(\alpha_2 - \delta)} = \frac{(U_{\rm PMNS})_{13} c_{13} c_{12}}{|(U_{\rm PMNS})_{11}| s_{13}}. \end{aligned} \tag{18}$$

The detailed calculation shown in Ref. [49], using the ISS relations, yields

$$m_D = z c_\beta \times \tilde{m}_D, \qquad \tilde{m}_D = \begin{pmatrix} 0 & x_{12} & x_{13} \\ -x_{12} & 0 & 1 \\ -x_{13} & -1 & 0 \end{pmatrix}, \tag{19}$$

where $z = \sqrt{2}vh^{\nu}_{23}$ is assumed to be positive and real,

$$x^*_{12} = \frac{(m_\nu)_{11}(m_\nu)_{23} - (m_\nu)_{13}(m_\nu)_{12}}{(m_\nu)_{12}(m_\nu)_{33} - (m_\nu)_{13}(m_\nu)_{23}}, \qquad x^*_{13} = \frac{(m_\nu)_{11}(m_\nu)_{33} - (m_\nu)^2_{13}}{(m_\nu)_{12}(m_\nu)_{33} - (m_\nu)_{13}(m_\nu)_{23}}. \tag{20}$$

We note that the lightest active neutrino mass is zero at the tree level, but can be nonzero when loop-corrections are included [38]. Also, the quantum effects can be considered for the charged lepton masses, so that the regions predicting large Δa_μ may be larger [58,59] than the ones discussed in this work. The perturbative limit requires that $h^{\nu}_{23} < \sqrt{4\pi}$, leading to the following upper bound of z,

$$z < 1233 \text{ [GeV]}. \tag{21}$$

The two formulas in Eq. (20) were found in the general symmetric from of M^{-1}, namely they are be found by using Eq. (12) for off-diagonal entries of m_ν to determine $(M^{-1})_{ij}$, then insert them into the diagonal ones. The off-diagonal elements of M^{-1} are determined as follows:

$$\begin{aligned}
(M^{-1})_{12} &= \frac{1}{2}\left[x^*_{13}(M^{-1})_{11} - \frac{(M^{-1})_{22}}{x^*_{13}} - \frac{(m_\nu)_{13} + x^*_{13}(m_\nu)_{23}}{x^*_{12}x^*_{13}z^2}\right], \\
(M^{-1})_{13} &= \frac{1}{2}\left[x^*_{12}(M^{-1})_{11} + \frac{(M^{-1})_{33}}{x^*_{12}} - \frac{(m_\nu)_{12} + x^*_{12}(m_\nu)_{23}}{x^*_{12}x^*_{13}z^2}\right], \\
(M^{-1})_{23} &= \frac{1}{2}\left[\frac{x^{*2}_{12}(M^{-1})_{22} - x^{*2}_{13}(M^{-1})_{33}}{x^*_{12}x^*_{13}} + \frac{x^*_{13}(m_\nu)_{12} - x^*_{12}(m_\nu)_{13}}{x^*_{12}x^*_{13}z^2}\right].
\end{aligned} \tag{22}$$

Hence all elements of the matrix M^{-1} depend on only three complex parameters $(M^{-1})_{ii}$ with $i = 1, 2, 3$. When identifying with $M^{-1} = (M^\dagger_R)^{-1}\mu_X(M^*_R)^{-1}$ given in Eq. (11), six parameters $\mu_{X,i}$ and $(M^{-1})_{ii}$ are determined as functions of elements of M_R. In this work, we will consider all elements of M_R are free parameters, namely

$$(M_R)_{ij} = zc_\beta \times (\widetilde{M}_R)_{ij}, (\widetilde{M}_R)_{ij} \equiv k_{ij}, \tag{23}$$

where all k_{ij} are assumed to be real for simplicity. The ISS relations are valid with at least some $|k_{ij}| \gg 1$ and $\det M \neq 0$. In the numerical investigation, m_ν is determined from the 3σ neutrino oscillation data through Eq. (12). The Dirac matrix m_D is then determined by Eq. (19). The free parameters k_{ij} and z are assumed to be real, and z is positive. The three elements of the matrix μ_X are determined as functions of these free parameters. The respective formulas are lengthy hence they are not written down explicitly here. In our work, we only consider the case $\max|\mu_{X,i}| \ll z$ hence all $(\mu_X)_i$ gives suppressed mixing elements in the total lepton mixing matrix U^ν. This condition will always be checked numerically to derive the final results.

In the numerical investigation, the free parameters z and k_{ij} will be scanned in the valid ranges to construct the total neutrino mass matrix defined in Eq. (7). After that, the mass eigenstates and the total mixing matrix are calculated numerically with at least 30 digits of precision. Using the relations listed in Eqs. (17) and (18), we reproduce all of the oscillation parameters Δm^2_{ij} and s^2_{ij} then force them satisfying the 3σ allowed data. This will help us to collect the allowed values of z and k_{ij} in evaluating the cLFV branching ratios and $(g-2)_\mu$ data. We emphasize that the regions of the parameter space in our numerical investigation are more general than those mentioned in Refs. [36,49].

The Lagrangian for quark masses was discussed previously [38]. Here, we just remind the reader that the Yukawa couplings of the top quark must satisfy the perturbative limit $h^u_{33} < \sqrt{4\pi}$, leading to a lower bound $v_2 > \frac{\sqrt{2}m_t}{\sqrt{4\pi}}$. Combining this with the relations in Eqs. (4) and (5) gives a lower bound $t_\beta \geq 0.3$, which will be used in the numerical discussion.

B. Higgs bosons

The Higgs potential used here respect the new lepton number defined in Ref. [38], namely

$$\begin{aligned}
V_h = &\sum_{S=\eta,\rho,\chi}[\mu^2_S S^\dagger S + \lambda_S(S^\dagger S)^2] + \lambda_{12}(\eta^\dagger\eta)(\rho^\dagger\rho) + \lambda_{13}(\eta^\dagger\eta)(\chi^\dagger\chi) + \lambda_{23}(\rho^\dagger\rho)(\chi^\dagger\chi) \\
&+ \tilde{\lambda}_{12}(\eta^\dagger\rho)(\rho^\dagger\eta) + \tilde{\lambda}_{13}(\eta^\dagger\chi)(\chi^\dagger\eta) + \tilde{\lambda}_{23}(\rho^\dagger\chi)(\chi^\dagger\rho) + \sqrt{2}\omega f(\epsilon_{ijk}\eta^i\rho^j\chi^k + \text{h.c.}),
\end{aligned} \tag{24}$$

where f is a dimensionless parameter, which $f\omega$ is the same as that used in previous works. The minimum conditions of the Higgs potential as well as the identification of the SM-like Higgs were discussed in detailed previously [54,60]. The model always contains a light CP even neutral Higgs boson identified with the SM-like Higgs boson confirmed experimentally. This Higgs boson gives suppressed contributions to $(g-2)_\mu$ hence we will ignore it from now on. The model contains two pairs of singly charged Higgs bosons $H^\pm_{1,2}$ and Goldstone bosons of the gauge bosons $W^\pm$ and $Y^\pm$, which are denoted as $G^\pm_W$ and $G^\pm_Y$, respectively. The masses of all charged Higgs bosons are [51,60,61] $m^2_{H^\pm_1} = (\frac{\tilde{\lambda}_{12}v^2}{2} + \frac{fw^2}{s_\beta c_\beta})$, $m^2_{H^\pm_2} = (v^2c^2_\beta + w^2)(\frac{\tilde{\lambda}_{23}}{2} + ft_\beta)$, and $m^2_{G^\pm_W} = m^2_{G^\pm_Y} = 0$. The relations between the original and mass eigenstates of the charged Higgs bosons are [60]

$$\begin{pmatrix}\eta^\pm\\ \rho^\pm_1\end{pmatrix} = \begin{pmatrix}-s_\beta & c_\beta\\ c_\beta & s_\beta\end{pmatrix}\begin{pmatrix}G^\pm_W\\ H^\pm_1\end{pmatrix},$$
$$\begin{pmatrix}\rho^\pm_2\\ \chi^\pm\end{pmatrix} = \begin{pmatrix}-s_\theta & c_\theta\\ c_\theta & s_\theta\end{pmatrix}\begin{pmatrix}G^\pm_Y\\ H^\pm_2\end{pmatrix}, \tag{25}$$

where $t_\theta = v_1/w$.

The model contains five CP-odd neutral scalar components. Three of them are Goldstone bosons of the neutral gauge bosons Z, Z' and X^0. The two remaining are physical states with masses $m^2_{a_1} = f(c_\beta s_\beta v^2 + \frac{\omega^2}{t_\beta}) + \frac{\tilde{\lambda}_{13}}{2}(s_\beta{}^2v^2 + \omega^2)$, $m^2_{a_2} = f(\frac{\omega^2}{c_\beta s_\beta} + c_\beta s_\beta v^2)$. As a consequence, the parameter f must be positive. In addition, f may be small so that charged Higgs boson masses can be around 1 TeV.

III. ANALYTIC FORMULAS FOR ONE LOOP CONTRIBUTIONS TO Δa_{e_a} AND CLFV DECAYS $e_b \to e_a\gamma$

All detailed steps for calculation to derive the couplings that give large one-loop contributions were presented in Ref. [49]. We just collect the final results related with this work. The condition $m_{e_b} > m_{e_a}$ is always used to define the one loop form factors $c^X_{(ab)R}$ and $c^X_{(ba)R}$ introduced in Ref. [62], which are different from our notations by a relative factor m_{e_b}.

The relevant Lagrangian of charged gauge bosons is

$$\mathcal{L}^{\ell nV} = \overline{\psi_{aL}}\gamma^\mu D_\mu \psi_{aL} \supset \frac{g}{\sqrt{2}}\sum_{i=1}^{9}\sum_{a=1}^{3}[U^{\nu*}_{ai}\overline{n_i}\gamma^\mu P_L e_a W^+_\mu + U^{\nu*}_{(a+3)i}\overline{n_i}\gamma^\mu P_L e_a Y^+_\mu], \tag{26}$$

corresponding to the following one-loop form factors:

$$c^W_{(ab)R} = \frac{eg^2}{32\pi^2 m^2_W}\sum_{i=1}^{9}U^\nu_{ai}U^{\nu*}_{bi}F_{LVV}\left(\frac{m^2_{n_i}}{m^2_W}\right),$$
$$c^W_{(ba)R} = \frac{eg^2 m_{e_a}}{32\pi^2 m^2_W m_{e_b}}\sum_{i=1}^{9}U^\nu_{bi}U^{\nu*}_{ai}F_{LVV}\left(\frac{m^2_{n_i}}{m^2_W}\right),$$
$$c^Y_{(ab)R} = \frac{eg^2}{32\pi^2 m^2_W}\sum_{i=1}^{9}U^\nu_{(a+3)i}U^{\nu*}_{(b+3)i}\frac{m^2_W}{m^2_Y}\times F_{LVV}\left(\frac{m^2_{n_i}}{m^2_Y}\right),$$
$$c^Y_{(ba)R} = \frac{eg^2 m_{e_a}}{32\pi^2 m^2_W m_{e_b}}\sum_{i=1}^{9}U^\nu_{(b+3)i}U^{\nu*}_{(a+3)i}\frac{m^2_W}{m^2_Y}\times F_{LVV}\left(\frac{m^2_{n_i}}{m^2_Y}\right), \tag{27}$$

where

$$F_{LVV}(x) = -\frac{10 - 43x + 78x^2 - 49x^3 + 4x^4 + 18x^3\ln(x)}{24(x-1)^4}, \tag{28}$$

$e = \sqrt{4\pi\alpha_{\rm em}}$ being the electromagnetic coupling constant, and $g = e/s_W$.

Lagrangian of charged Higgs bosons is

$$\mathcal{L}^{\ell nH} = -\frac{g}{\sqrt{2}m_W}\sum_{k=1}^{2}\sum_{a=1}^{3}\sum_{i=1}^{9}H^+_k\overline{n_i}(\lambda^{L,k}_{ai}P_L + \lambda^{R,k}_{ai}P_R)e_a + \text{H.c.}, \tag{29}$$

where

$$\lambda^{R,1}_{ai} = m_{e_a}U^{\nu*}_{ai}t_\beta, \qquad \lambda^{R,2}_{ai} = \frac{m_{e_a}c_\theta U^{\nu*}_{(a+3)i}}{c_\beta},$$
$$\lambda^{L,1}_{ai} = -t_\beta\sum_{c=1}^{3}(m^*_D)_{ac}U^\nu_{(c+3)i} = -s_\beta z\sum_{c=1}^{3}(\tilde{m}^*_D)_{ac}U^\nu_{(c+3)i},$$
$$\lambda^{L,2}_{ai} = \sum_{c=1}^{3}\frac{c_\theta}{c_\beta}\times[(m^*_D)_{ac}U^\nu_{ci} + t^2_\theta(M^*_R)_{ac}U^\nu_{(c+6)i}] = c_\theta z\sum_{c=1}^{3}[(\tilde{m}^*_D)_{ac}U^\nu_{ci} + t^2_\theta(\tilde{M}^*_R)_{ac}U^\nu_{(c+6)i}]. \tag{30}$$

The one-loop form factors are

$$c^{H,k}_{(ab)R} = \frac{eg^2}{32\pi^2 m_W^2 m_{e_b} m^2_{H_k}} \sum_{i=1}^{9} \left[\lambda^{L,k*}_{ai} \lambda^{R,k}_{bi} m_{n_i} F_{LHH}\left(\frac{m^2_{n_i}}{m^2_{H_k}}\right) + (m_{e_b} \lambda^{L,k*}_{ai} \lambda^{L,k}_{bi} + m_{e_a} \lambda^{R,k*}_{ai} \lambda^{R,k}_{bi}) \tilde{F}_{LHH}\left(\frac{m^2_{n_i}}{m^2_{H_k}}\right) \right],$$
$$c^{H,k}_{(ba)R} = \frac{eg^2}{32\pi^2 m_W^2 m_{e_b} m^2_{H_k}} \sum_{i=1}^{9} \left[\lambda^{L,k*}_{bi} \lambda^{R,k}_{ai} m_{n_i} F_{LHH}\left(\frac{m^2_{n_i}}{m^2_{H_k}}\right) + (m_{e_a} \lambda^{L,k*}_{bi} \lambda^{L,k}_{ai} + m_{e_b} \lambda^{R,k*}_{bi} \lambda^{R,k}_{ai}) \tilde{F}_{LHH}\left(\frac{m^2_{n_i}}{m^2_{H_k}}\right) \right], \quad (31)$$

where $b \geq a$, and

$$F_{LHH}(x) = -\frac{1 - x^2 + 2x\ln(x)}{4(x-1)^3}, \qquad \tilde{F}_{LHH}(x) = -\frac{-1 + 6x - 3x^2 - 2x^3 + 6x^2\ln(x)}{24(x-1)^4}. \quad (32)$$

The total one-loop contribution to the cLFV and $\Delta a_\mu^{331\text{ISS}}$ is

$$c_{(ab)R} = c^W_{(ab)R} + c^Y_{(ab)R} + c^{H_1}_{(ab)R} + c^{H_2}_{(ab)R}, \qquad c_{(ba)R} = \{c_{(ab)R}[a \leftrightarrow b]\} \times \frac{m_{e_a}}{m_{e_b}}. \quad (33)$$

The one-loop contributions from charged gauge bosons to the a_{e_a} and the electric dipole moment d_{e_a} of the charged lepton e_a are [62]:

$$a^V_{e_a} = a^W_{e_a} + a^Y_{e_a} \equiv -\frac{4m^2_{e_a}}{e}(\text{Re}[c^W_{(aa)R}] + \text{Re}[c^Y_{(aa)R}]),$$
$$d^V_{e_a} = d^W_{e_a} + d^Y_{e_a} \equiv -2m_{e_a}(\text{Im}[c^W_{(aa)R}] + \text{Im}[c^Y_{(aa)R}]), \quad (34)$$

The one-loop contribution to a_{e_a} and d_{e_a} caused by charged Higgs bosons is [62]:

$$a^H_{e_a} = \sum_{k=1}^{2} a^{H,k}_{e_a}, \qquad a^{H,k}_{e_a} \equiv -\frac{4m^2_{e_a}}{e}\text{Re}[c^{H,k}_{(aa)R}],$$
$$d^H_{e_a} = \sum_{k=1}^{2} d^{H,k}_{e_a}, \qquad d^{H,k}_{e_a} \equiv -2m_{e_a}\text{Im}[c^{H,k}_{(aa)R}]. \quad (35)$$

The quantity $\Delta d_{e_a} = d^V_{e_a} + d^H_{e_a}$ is the new one loop contributions predicted to the electric dipole moment of the charged leptons. It equals to zero when our investigation is limited in the case of the Dirac phase $\delta = \pi$. This zero value of d_μ satisfies the current experimental constraint [63] hence we will not consider from now on.

We remind the reader that one loop contributions from neutral Higgs bosons are very suppressed hence they are ignored here. The reason is that the 331ISS model has no new charged leptons, hence the one-loop contributions of any neutral Higgs bosons H^0 to $c_{(ab)R}$ must arise only from the couplings $H^0\bar{e}_a e_a$ derived from the first term of the Yukawa Laragian (6). These couplings have the same Yukawa couplings with the SM-like $h \sim \text{Re}[\rho^0]/\sqrt{2}$, but different mixing factors $|c_{H^0}| \leq 1$ telling the contributions of ρ^0 to the physical state H^0. Hence these contributions to a_μ have the same form with the one from the SM-like Higgs boson having mass $m_h \simeq 125$ GeV $\gg m_\mu$, $a^h_\mu \simeq \frac{\sqrt{2}G_\mu m^2_\mu}{4\pi^2} \times \frac{m^2_\mu}{m^2_h}\ln\frac{m^2_h}{m^2_\mu} \leq \mathcal{O}(10^{-14})$ [64]. Also, the heavy neutral Higgs will give suppressed one-loop contributions to Δa_μ. The deviation of a_μ between predictions by the two models 331ISS and SM are

$$\Delta a^{331\text{ISS}}_{e_a} \equiv \Delta a_{e_a} = \Delta a^W_{e_a} + a^Y_{e_a} + a^{H,1}_{e_a} + a^{H,2}_{e_a},$$
$$\Delta a^W_{e_a} = a^W_{e_a} - a^{\text{SM},W}_{e_a}, \quad (36)$$

where $a^{\text{SM},W}_\mu = 3.887 \times 10^{-9}$ [64] is the SM prediction for the one-loop contribution from W boson $c^{W,\text{SM}}_{(22)R}$. In this work, $\Delta a^{331\text{ISS}}_\mu = \Delta a_\mu$ will be considered as new physics predicted by the 331ISS and will be used to compare with the experimental data in the following numerical investigation. We note that the discrepancy of a_e between experiments and SM is about 2.5 standard deviation [3,20,65–68]. In this work we will only pay attention to the Δa_μ which is the very interesting result of 4.2 standard

TABLE I. Constraints of $c_{(ab)R}[\mathrm{GeV}^{-2}]$ from experimental data. The allowed values of Δa_μ satisfying a confidence level of 1σ from the experimental data given in Eq. (1).

$192 < \Delta a_\mu \times 10^{11} < 310$, -4.8×10^{-8} $[\mathrm{GeV}^{-2}] < c_{(22)R} < -3.99 \times 10^{-8}$ $[\mathrm{GeV}^{-2}]$	
$\mathrm{Br}(\mu \to e\gamma)$	$\lvert c_{(21)R}\rvert, \lvert c_{(12)R}\rvert < 3.47 \times 10^{-13}$ $[\mathrm{GeV}^{-2}]$
$\mathrm{Br}(\tau \to e\gamma)$	$\lvert c_{(31)R}\rvert, \lvert c_{(13)R}\rvert < 2.31 \times 10^{-10}$ $[\mathrm{GeV}^{-2}]$
$\mathrm{Br}(\tau \to \mu\gamma)$	$\lvert c_{(32)R}\rvert, \lvert c_{(23)R}\rvert < 2.63 \times 10^{-10}$ $[\mathrm{GeV}^{-2}]$

deviation and may be a clear signal of new physics in the near future.

Based on Ref. [62], the branching ratios of the cLFV processes are

$$\mathrm{Br}(e_b \to e_a\gamma) \simeq \frac{48\pi^2}{G_F^2}(|c_{(ab)R}|^2 + |c_{(ba)R}|^2)\mathrm{Br}(e_b \to e_a\overline{\nu_a}\nu_b), \tag{37}$$

where $G_F = g^2/(4\sqrt{2}m_W^2)$. This result is consistent with the formulas given used in Refs. [49,61] for $3-3-1$ models.

It is noted that for the gauge boson contributions, we have $|c^V_{(ba)R}|/|c^V_{(ab)R}| = m_{e_a}/m_{e_b} \ll 1$ for $m_{e_b} > m_{e_a}$. Similarly, we can estimate that $|c^{H,k}_{(ba)R}|/|c^{H,k}_{(ab)R}| \ll 1$ for every particular contribution. Anyways, in the general case we cannot ignore $c^X_{(ba)R}$ because of the situation that when contributions to $c_{(ab)R}$ have the same order but some of them have opposite signs. Then the very destructive correlations among particular Higgs contributions in the $c_{(ab)R}$ will result in the same order of both $|c_{(ab)R}|$ and $|c_{(ba)R}|$. This will happen in the 331ISS model when $\Delta a_\mu^{331\mathrm{ISS}} = \mathcal{O}(10^{-9})$ corresponding to the order of the experimental data and $\mathrm{Br}(\mu \to e\gamma) < 4.2 \times 10^{-13}$ require both conditions of $\mathcal{O}(10^{-9})$ $[\mathrm{GeV}^{-2}] \leq |c_{(22)R}| \leq \mathcal{O}(10^{-8})$ $[\mathrm{GeV}^{-2}]$ and $|c_{(21)R}| \leq \mathcal{O}(10^{-13}) \times$ $[\mathrm{GeV}^{-2}]$, respectively. As a result, we can estimate that the one-loop contributions from two charged Higgs bosons to $\mathrm{Br}(\mu \to e\gamma)$ are strongly destructive, i.e., $c^{H_1}_{(12)} \simeq -c^{H_2}_{(12)}$. Simultaneously, $|c^{H_k}_{(12)}| \sim |c^{H_k}_{(22)}|$, therefore the charged Higgs contributions to Δa_μ must be constructive and satisfy $|c^{H_1}_{(22)}| \sim |c^{H_2}_{(22)}| \sim \mathcal{O}(10^{-9}) - \mathcal{O}(10^{-8})$ $[\mathrm{GeV}^{-2}]$, or they can be destructive but $|c^{H_i}_{(22)}| \gg |c^{H_j}_{(22)}|$ with $i \neq j$. These important properties of charged Higgs boson contributions will be the key point in our numerical investigation to collect data points satisfying the large values of $\Delta a_\mu \geq 10^{-9}$ before considering any cLFV decay constraints. The gauge contributions are suppressed hence we do not discuss qualitatively here, but they are also included in the numerical investigation. We just pay attention to the two key one-loop charged Higgs boson contributions which will affect two other cLFV decays $\tau \to e\gamma, \mu\gamma$.

The experimental constraints of the form factors $c_{(ab)R}$ are listed in Table I, where the allowed values of Δa_μ are chosen in the range of 1σ confidence level given in Eq. (1). We derive that the allowed regions of the parameter space have the following properties:

$$\left|\frac{c_{(12)R}}{c_{(22)R}}\right|, \left|\frac{c_{(21)R}}{c_{(22)R}}\right| \leq \mathcal{O}(10^{-5});$$
$$\left|\frac{c_{(13)R}}{c_{(22)R}}\right|, \left|\frac{c_{(31)R}}{c_{(22)R}}\right|, \left|\frac{c_{(23)R}}{c_{(22)R}}\right|, \left|\frac{c_{(32)R}}{c_{(22)R}}\right| \leq \mathcal{O}(10^{-2}). \tag{38}$$

Normally, our numerical scan gives a relation that $|c^{H_k}_{(22)R}|/|c^{H_k}_{(ab)R}| \leq \mathcal{O}(10)$ with $a \neq b$. As a result, the huge destructive correlation between charged Higgs contributions to guarantee simultaneously the experimental constraints of $\mathrm{Br}(\mu \to e\gamma)$ and Δa_μ. Also, the two cLFV decays of $\tau \to e\gamma, \mu\gamma$ also need smaller but still large destructive charged Higgs contributions to satisfy the upper experimental bounds because some of these particular contributions often satisfy $|c^{H_k}_{(13)R}|/|c^{H_k}_{(22)R}|, |c^{H_k}_{(23)R}|/|c^{H_k}_{(22)R}| \geq 0.1$. While $|c^{H_k}_{(31)R}|, |c^{H_k}_{(32)R}| \ll 10^{-10}$ $[\mathrm{GeV}^{-2}]$, consequently they are subdominant to the cLFV decays where their branching ratios are close to the upper experimental constraints. The mentioned properties are very important for us to point out the validation of the allowed regions.

For convenience in estimating qualitatively the above properties, we define new important quantities determining the correlations between two charged Higgs contributions in a physical process as follows:

$$R^X_{ab} \equiv \left|\frac{\mathrm{Re}[c^X_{(ab)R}]}{\mathrm{Re}[c_{(ab)R}]}\right|; \quad a,b = 1,2,3; \quad X = W, Y, H_1^\pm, \quad H_2^\pm, \tag{39}$$

$$R^-_{ab} \equiv \left|\frac{\mathrm{Re}[c^{H_1}_{(ab)R} + c^{H_2}_{(ab)R}]}{\mathrm{Re}[c_{(ab)R}]}\right|. \tag{40}$$

The first ratio R^X_{ab} shows the relative contribution from the particle X in the loop to the total contribution. The second one shows the relative contributions of both singly charged Higgs bosons. In the 331ISS model, we will see that the relations $R^W_{ab}, R^Y_{ab} \ll R^{H_k}_{ab}$ often happens. The interesting possibility we would like to discuss is that large contributions of H_k for large Δa_μ with $|R^{H_k}_{22}| \sim 10^{-1}$, while the huge destructive correlations of these two Higgs bosons $\mathrm{Re}[c^{H_1}_{(ab)R}/c^{H_2}_{(ab)R}] \simeq -1$ will allow small cLFV constraints. Quantitatively, we estimate that $R^{H_k}_{ab} \gg 1$ and $R^{-}_{ab} \simeq 1$, with $a \neq b$. The details of numerical investigation will be shown below.

IV. ADDITIONAL SINGLY CHARGED HIGGS BOSON FOR AN EXPLANATION OF $(g-2)_\mu$ DATA AT 1σ DEVIATION

The appearance of the gauge singlet X_R leads to a possibility that, a new singly charged Higgs bosons $h_3^\pm \sim (1,1,\pm 1)$ can be included in the 331ISS model so that they can give one-loop contributions to both Δa_μ and cLFV amplitudes through the following Yukawa interactions:

$$\begin{aligned}\mathcal{L}^Y_{h_3} &= -Y^3_{ab}\overline{(X_{aR})^c}e_{bR}h_3^+ + \mathrm{H.c.}\\ &= -Y^3_{ab}U^{\nu *}_{(a+6)i}\overline{(n_i)}P_R e_b h_3^+ + \mathrm{H.c.}.\end{aligned} \tag{41}$$

The new contributions to the cLFV decays and $\Delta a_\mu^{331\mathrm{ISS}}$ is

$$\begin{aligned}c^{h_3}_{(ab)R} &= \frac{em_{e_a}}{16\pi^2 m_{e_b} m^2_{h_3}}\sum_{i=1}^{9}\sum_{c=1}^{3} Y^3_{ca}Y^{3*}_{cb}U^{\nu *}_{(a+6)i}U^{\nu}_{(b+6)i}\tilde{F}_{LHH}\left(\frac{m^2_{n_i}}{m^2_{h_3}}\right),\\ c^{h_3}_{(ba)R} &= \frac{e}{16\pi^2 m^2_{h_3}}\sum_{i=1}^{9}\sum_{c=1}^{3} Y^{3*}_{ca}Y^{3}_{cb}U^{\nu}_{(a+6)i}U^{\nu *}_{(b+6)i}\tilde{F}_{LHH}\left(\frac{m^2_{n_i}}{m^2_{h_3}}\right).\end{aligned} \tag{42}$$

Although the contributions of these singly charged Higgs bosons to Δa_μ are normally small and negative, the contributions to the cLFV amplitudes may be significantly large. Consequently, they can affect destructively the total cLFV decay amplitudes. These properties will keep $\Delta a_\mu^{331\mathrm{ISS}}$ reaching the experimental constraint given in Eq. (1), while keeping all other cLFV branching ratios well below the experimental constraints. In this work, we consider the simplest case that $h_3^\pm$ does not mix with the other singly charged Higgs bosons in the 331RN, and the mass is another free parameter. All of these properties can be derived easily from the total Higgs potential, hence it will be ignored in this work.

V. NUMERICAL DISCUSSION

A. Without contributions from additional singly charged Higgs bosons $h_3^\pm$

The numerical experimental parameters are taken from Ref. [4]:

$$\begin{aligned}&G_F = 1.663787\times 10^{-5}\ \mathrm{GeV}^{-2}, \quad g = 0.652, \quad \alpha_e = \frac{1}{137} = \frac{e^2}{4\pi}, \quad s^2_W = 0.231, \quad m_e = 5\times 10^{-4}\ \mathrm{GeV},\\ &m_\mu = 0.105\ \mathrm{GeV}, \quad m_\tau = 1.776\ \mathrm{GeV}, \quad m_W = 80.385\ \mathrm{GeV},\\ &\mathrm{Br}(\mu \to e\bar{\nu}_e\nu_\mu) \simeq 1., \quad \mathrm{Br}(\tau \to e\bar{\nu}_e\nu_\tau) \simeq 0.1782, \quad \mathrm{Br}(\tau \to \mu\bar{\nu}_\mu\nu_\tau) \simeq 0.1739.\end{aligned} \tag{43}$$

Before discussing on the allowed regions that satisfy all experimental constraints of cLFV decays $e_b \to e_a\gamma$ as well as $(g-2)_\mu$ data, we give some important crude estimation on the allowed regions of parameter space constrained by both large $\Delta a_\mu^{331\mathrm{ISS}} \geq \mathcal{O}(10^{-9})$ and small $\mathrm{Br}(e_b \to e_a\gamma)$. The way to derive the total mass matrix to calculate numerically the masses and total neutrino mixing matrix U^ν were presented in the previous section. We have checked that the input changes of Δm^2_{ij} and s^2_{ij} in the allowed ranges given in Eq. (16) do not change significantly the final results, so we will fix these quantities at their best-fit points. An exception that the Dirac phase $\delta = 180$ [Deg.] is considered so that the imagine parts of $c_{(ab)R}$ are zeros, leading to a simple case of destruction among the one-loop contributions from charged Higgs bosons.

In the numerical scan, the points in the allowed regions also satisfy simultaneously the following conditions:

(1) The condition $\mathrm{Re}[c^{H_1}_{(ab)R}]/\mathrm{Re}[c^{H_2}_{(ab)R}] < 0$ with $a \neq b$, will give a possibility that $\mathrm{Re}[c^{H_1}_{(21)R}] + \mathrm{Re}[c^{H_2}_{(21)R}] \sim 0$, which will result in valid regions of the parameter space in which two charged Higgs bosons contributions can cancel each others.

Therefore, these regions will contain points which give the very suppressed total contributions to guarantee the small $\mathrm{Br}(e_b \to e_a\gamma)$. We will use this condition in our numerical investigation.

(2) A crude numerical scan shows that the condition $\mathrm{Re}[c^{H_1}_{(22)R}]/\mathrm{Re}[c^{H_2}_{(22)R}] > 0$ so that the two charged Higgs bosons contributions to $\Delta a_\mu^{331\mathrm{ISS}}$ always have the same sign, i.e., they give constructive contributions. Therefore the values of $\Delta a_\mu^{331\mathrm{ISS}}$ are remained in the original orders of $\mathcal{O}(10^{-9})$. Another case giving large Δa_μ is that $|\mathrm{Re}[c^{H_i}_{(22)R}]| \ll |\mathrm{Re}[c^{H_j}_{(22)R}]|$ with $i \neq j$ when they have opposite signs.

First, we consider the simplest cases of all zero values of off-diagonal elements $k_{ij} = 0$ with $i \neq j$. The numerical investigation shows that we cannot obtain any allowed points satisfying simultaneously both experimental data of cLFV constraints and Δa_μ. The reason is that there always exists a strict relation that $\mathrm{Re}[c^{H_1}_{(22)R}]/\mathrm{Re}[c^{H_2}_{(22)R}]$ and $\mathrm{Re}[c^{H_1}_{(21)R}]/\mathrm{Re}[c^{H_2}_{(21)R}]$ are always negative leading to small $\mathrm{Br}(\mu \to e\gamma)$. As a consequence, charged Higgs contributions to $\Delta a_\mu^{331\mathrm{ISS}}$ are always destructive. Hence, the derived values are smaller than the experimental data. A requirement of $\mathrm{Br}(\mu \to e\gamma) \leq \mathcal{O}(10^{-8})$ gives largest values of $\Delta a_\mu^{331\mathrm{ISS}} < 10^{-9}$.

From a crude numerical scan, we can find the allowed regions of the parameter space satisfying both conditions that $\mathrm{Br}(\mu \to e\gamma) < 4.2 \times 10^{-13}$ and large $\Delta a_\mu^{331\mathrm{ISS}} \geq \mathcal{O}(10^{-9})$. These allowed regions will be used to collect the allowed points satisfying the remaining cLFV constraints. The following ranges of the parameter space will be chosen as the necessary conditions of free parameters when scanning to collect allowed points:

$$\begin{aligned} &t_\beta \in [0.3, 60], 0.6\ [\mathrm{TeV}] \leq m_{H_1}, \quad && m_{H_2} \leq 3\ [\mathrm{TeV}], \\ &|k_{ij}| \times z c_\beta < \sqrt{4\pi} w = 5.3\ [\mathrm{TeV}], && 10\ [\mathrm{GeV}] \leq z \leq 1223\ [\mathrm{TeV}]. \end{aligned} \tag{44}$$

Numerical values of k_{ij} will be chosen so that they give active neutrino masses and U_{PMNS} consistent with neutrino oscillation data. The value of 5.3 TeV is fixed from the lower bound w obtained from the experimental data of the heavy Z' boson mass $m_{Z'}$. But it can be relaxed with larger w without any changes of final conclusions in this work.

Without contributions of the additional singly charged Higgs boson, our numerical investigation shows that the largest values of Δa_μ satisfying all cLFV constraints is $\Delta a_\mu \leq 108.5 \times 10^{-11}$, see an illustration shown in Fig. 1. The corresponding ranges of the free parameters are shown in Table II, where the right panel shows the only contributions from $c_{(ab)R}$ $(a < b)$ to the decay rates, namely

$$\mathrm{Br}(abR) = \frac{48\pi^2}{G_F^2}|c_{(ab)R}|^2 \mathrm{Br}(e_b \to e_a \overline{\nu_a} \nu_b).$$

Here the two first lines show the respective minimum and maximum values of the free parameters. The third line shows a particular example of the set of the parameters giving large $\Delta a_\mu \simeq 108.1 \times 10^{-11}$. The other quantities are shown in Table III, which will be discussed more later.

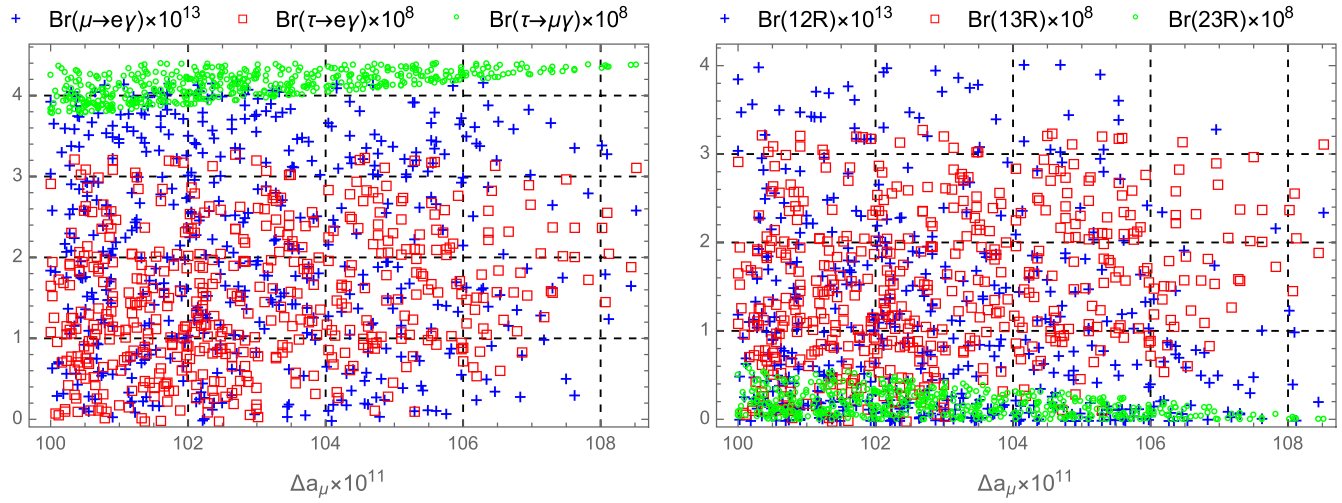

FIG. 1. The left panel shows Δa_μ vs $\mathrm{Br}(e_b \to e_a\gamma) \sim (|c_{(ab)R}|^2 + |c_{(ba)R}|^2)$ in the free parameter ranges given in Table II. The right panel shows $\mathrm{Br}(abR) \sim |c_{(ab)R}|^2$ with $a < b$.

TABLE II. Numerical values of free parameters for large $\Delta a_\mu^{331\text{ISS}} \geq 10^{-9}$ satisfying all experimental constraints of the cLFV decays $e_b \to e_a\gamma$.

Notation	k_{11}	k_{22}	k_{33}	k_{12}	k_{13}	k_{23}	k_{21}	k_{31}	k_{32}	t_β	z [GeV]	m_{H_1}[GeV]	m_{H_2}[GeV]
Min	−3.99	−50.2	509.	−29.9	15.4	−80.4	121.	21.2	29.4	29.0	885.	705	769
Max	2.47	−35.1	528.	−20.6	24.9	−66.4	135.	36.8	45.9	40.0	1150	893	962
Example	−3.26	−49.7	509.	−28.6	23.0	−77.8	124.	25.3	37.1	36.9	969.	754	825

In the left panel of Fig. 1, only $\text{Br}(\tau \to \mu\gamma)$ always enhances with increasing Δa_μ. The upper constraint $\text{Br}(\tau \to \mu\gamma) < 4.4 \times 10^{-8}$ gives the largest value of $\Delta a_\mu \simeq 108.5 \times 10^{-11}$. From the right panel of Fig. 1, we see that $|c_{(23)R}| < |c_{(32)R}|$ in the region predicting large Δa_μ, because the contribution from $|c_{(23)R}|$ to $\text{Br}(\tau \to \mu\gamma)$ denoted as $\text{Br}(23R)$ is small, namely $\text{Br}(23R) \leq 0.2 \times 10^{-8}$ with $\Delta a_\mu \geq 108 \times 10^{-11}$. This is in contrast to other normal cases, as we will discuss based on the Table III.

Table III illustrates particular values of $c_{(ab)R}$ and large $\Delta a_\mu^{331\text{ISS}} \simeq 108.1 \times 10^{-11}$, corresponding to a set of free parameters given in the third line of Table II. The numerical results given in Table III show that the experimental constraint from $\text{Br}(\tau \to \mu\gamma) < 4.4 \times 10^{-8}$ does not allow large $\Delta a_\mu^{331\text{ISS}} > 108.5 \times 10^{-11}$. More particular, $c_{(32)R}$ gives the dominant contribution to $\text{Br}(\tau \to \mu\gamma) < 4.4 \times 10^{-8}$, with $|c_{(32)R}^{H_2}| \gg |c_{(32)R}^{H_1}|$. In contrast, the remaining cLFV decays have some common properties that $|c_{(ab)R}| > |c_{(ba)R}|$ with $a < b$, $|c_{(ab)R}^{H_k}| \gg |c_{(ab)R}|$, and the huge destructive correlation between two charged Higgs boson contributions. They are very important to guarantee small $\text{Br}(\tau \to e\gamma)$ and $\text{Br}(\mu \to e\gamma)$. On the other hand, they allow large and/or constructive $c_{(22)R}^{H_k}$, which are the dominant contributions resulting in large $\Delta a_\mu^{331\text{ISS}} \geq 10^{-9}$.

The above properties are also true for the allowed region of the parameter space given in Table II. They are summarized in Table IV through the quantities defined in Eqs. (39) and (40). We can see that $R_{32}^- = |\text{Re}[c_{(32)R}^{H_2} + c_{(32)R}^{H_1}]/\text{Re}[c_{(32)R}]| \to 1$ implies that sum of the two contributions of the charged Higgs bosons to $c_{(32)R}$ is dominant. In addition $R_{32}^{H_2} \equiv |\text{Re}[c_{(32)R}^{H_2}]/\text{Re}[c_{(32)R}]| \simeq 1$ indicates that the contributions of the charged Higgs boson H_2 is dominant, hence the destructive correlation is small. This is not enough to keep the cLFV constraint $\text{Br}(\tau \to \mu\gamma) < 4.4 \times 10^{-8}$ for larger $\Delta a_\mu > 108.5 \times 10^{-11}$. All contributions of the two decays $\mu \to e\gamma$ and $\tau \to e\gamma$ do not have properties mentioned here. In the next discussion, we will show that new destructive contributions from additional

TABLE III. Particular contributions $c_{(ab)R}^X[\text{GeV}^{-2}]$ to the Δa_μ and $\text{Br}(e_b \to e_a\gamma)$ with the free parameters given in the third line of Table II. The last column shows values of Δa_μ and $\text{Br}(e_b \to e_a\gamma)$.

Notations	$c_{(ab)R}^W - c_{(ab)R}^{W,\text{SM}}$	$c_{(ab)R}^Y$	$c_{(ab)R}^{H_1}$	$c_{(ab)R}^{H_2}$	$c_{(ab)R}$	Process
$\Delta a_\mu : c_{(22)R} \times 10^{10}$	5.22	−0.499	−82.07	3.11	−74.24	$\Delta a_\mu = 10.81 \times 10^{-10}$
$\mu \to e\gamma : c_{(12)R} \times 10^{13}$	422.13	29.645	−29086.	28636.	1.6960	$\text{Br}(12R) = 1.002 \times 10^{-13}$
$\mu \to e\gamma : c_{(21)R} \times 10^{13}$	2.010	0.1412	−138.5	138.9	2.568	$\text{Br}(21R) = 2.296 \times 10^{-13}$
$\tau \to e\gamma : c_{(13)R} \times 10^{10}$	−0.031	0.01941	13.60	−15.63	−2.039	$\text{Br}(13R) = 257.9 \times 10^{-10}$
$\tau \to e\gamma : c_{(31)R} \times 10^{10}$	≃0	≃0	0.004	0.031	0.035	$\text{Br}(31R) = 0.076 \times 10^{-10}$
$\tau \to \mu\gamma : c_{(23)R} \times 10^{10}$	−0.02505	−0.03235	−0.3305	0.5170	0.1291	$\text{Br}(23R) = 1.009 \times 10^{-10}$
$\tau \to \mu\gamma : c_{(32)R} \times 10^{10}$	−0.001481	−0.001913	−0.01954	−2.656	−2.679	$\text{Br}(32R) = 434.7 \times 10^{-10}$

TABLE IV. Correlations between different contributions to $c_{(ab)R}$ with ranges of free parameters given in Table II, where we denote $0 \simeq R_{(22)R}^Y, R_{(31)R}^W, R_{(31)R}^Y, R_{(32)R}^W, R_{(32)R}^Y \leq \mathcal{O}(10^{-3})$.

	R_{22}^W	$R_{22}^{H_1}$	$R_{22}^{H_2}$	R_{12}^W	R_{12}^Y	$R_{12}^{H_1}$	$R_{12}^{H_2}$	R_{12}^-	R_{21}^W	R_{21}^Y	$R_{21}^{H_1}$	$R_{21}^{H_2}$	R_{21}^-	R_{13}^W	R_{13}^Y
Min	0.06	0.96	0	54	7	$\sim 10^3$	$\sim 10^3$	60	0.3	0.04	34	34	0.01	0.01	0
Max	0.08	1.11	0.1	$\sim 10^5$	$\sim 10^4$	$\sim 10^7$	$\sim 10^7$	$\sim 10^6$	299	37	$\sim 10^4$	$\sim 10^4$	336	4.	3
	$R_{13}^{H_1}$	$R_{13}^{H_2}$	R_{13}^-	$R_{31}^{H_1}$	$R_{31}^{H_2}$	R_{31}^-	R_{23}^W	R_{23}^Y	$R_{23}^{H_1}$	$R_{23}^{H_2}$	R_{23}^-	$R_{32}^{H_1}$	$R_{32}^{H_2}$	R_{32}^-	
Min	6	7	0.05	0.1	0.8	≃1	0.01	0.03	0.5	0	0.02	0	0.96	0.998	
Max	$\sim 10^3$	$\sim 10^3$	2.6	0.2	0.89	≃1	16.4	15.4	222	255	33	0.04	0.996	1.002	

singly charged Higgs bosons will relax the sum of the contributions from two charged Higgs bosons $H_{1,2}$ to a larger values, while allow both $\Delta a_\mu^{331\text{ISS}}$ and $\text{Br}(\tau \to \mu\gamma)$ satisfying the experimental constraints given in Eqs. (1) and (2).

From the above discussion, we can see that $\max[\Delta a_\mu] \simeq 108.5 \times 10^{-11}$ predicted by the 331ISS model comes from the experimental constraints $\text{Br}(\tau \to \mu\gamma) < 4.4 \times 10^{-8}$, which gets main contributions from $c_{(32)R}$. On the other hand, $\text{Br}(\tau \to e\gamma)$ can reach to zero for large $\Delta a_\mu \geq 10^{-9}$, which is different from the normal behave of these two branching ratios $\text{Br}(\tau \to \mu\gamma) \sim \text{Br}(\tau \to e\gamma) \sim |c_{(23)R}|^2$, $|c_{(13)R}|^2 \gg |c_{(32)R}|^2, |c_{(31)R}|^2$. After some numerical checks, we see that the this difference is originated mainly from the following property: each quantity $\text{Br}(\tau \to \mu\gamma)$ or $\text{Br}(\tau \to e\gamma)$ contains only one type of terms with a factor $\frac{m_\mu}{m_\tau}$ or $\frac{m_e}{m_\tau}$ appearing in $c_{(32)R}$ or $c_{(31)R}$, respectively. These terms are normally suppressed because of many other large terms contained in $c^{H_k}_{(23)R}, c^{H_k}_{(13)R} \gg c^{H_k}_{(32)R}, c^{H_k}_{(31)R}$. But when huge destructive correlations between two charged Higgs contributions and gauge contributions happen, there appears a situation that $|c_{(13)R}|, |c_{(23)R}| \to 0$, and also for other normal large terms in $|c_{(31)R}|, |c_{(32)R}|$. Now, the terms with factors $\frac{m_\mu}{m_\tau}$ and $\frac{m_e}{m_\tau}$ become significant, leading to the consequence that $\text{Br}(\tau \to e\gamma) \sim \frac{m_e^2}{m_\tau^2}$ can be close to 0, while $\text{Br}(\tau \to \mu\gamma) \sim \frac{m_\mu^2}{m_\tau^2} \gg \text{Br}(\tau \to e\gamma)$. It is reasonable to think that the terms with factor $\frac{m_\mu}{m_\tau}$ and $\Delta a_\mu^{331\text{ISS}}$ get similar contributions relating to μ, hence both of them must be large if $\Delta a_\mu^{331\text{ISS}}$ is required to be large in order to reach the experimental constraints. Our explanation is confirmed by a numerical check, where we change $m_\mu \to m_e$ in only the formula of $c_{(32)R}$. We saw that $\text{Br}(\tau \to \mu\gamma, e\gamma)$ can reach small values $\text{Br}(\tau \to \mu\gamma, e\gamma) < 10^{-9}$ with $\Delta a_\mu^{331\text{ISS}} > 125 \times 10^{-11}$. Other numerical checks also show that the lower bound of $\text{Br}(\tau \to \mu\gamma)$ depends strictly on the lepton mixing matrix U_{PMNS}, which is the only cLFV source in the 331ISS model. First, the case of large $\tau - e$ mixing inputs $s_{13}^2 = s_{23}^2 = 0.547$ can give large $\Delta a_\mu^{331\text{ISS}} > 115 \times 10^{-11}$ and both small $\text{Br}(\tau \to \mu\gamma, e\gamma) \to 0$. Second, the small input $s_{23}^2 = 0.0216$ and the large input $s_{13}^2 = 0.547$ will result in that $\max[\Delta a_\mu^{331}] \simeq 90 \times 10^{-11}$. In both cases, $\max[\Delta a_\mu^{331\text{ISS}}]$ is still constrained by $\text{Br}(\tau \to \mu\gamma) < 4.4 \times 10^{-8}$. In conclusion, the regions of the parameter space giving $\max[a_\mu^{331\text{ISS}}]$ allows all small $c_{(ab)R}$ except the terms with factor $\frac{m_\mu}{m_\tau}$ in $c_{(32)R}$.

B. New contributions from additional singly charged Higgs bosons $h_3^\pm$

Adding contributions of the new singly charged Higgs boson, the allowed values of $\Delta a_\mu \equiv \Delta a_\mu^{331\text{ISS}} \geq 192 \times 10^{-11}$ corresponding to the lower bound of the 1σ confidence level are explained successfully, see an illustration shown in Fig. 2, where $\Delta a_\mu(h_3)$ and $\text{Br}(\tau \to \mu\gamma)[h_3]$ show the respective one-loop contributions from only $h_3^\pm$ to Δa_μ and $\text{Br}(\tau \to \mu\gamma)$, which are defined as follows:

$$\Delta a_\mu[h_3] = -\frac{4m_\mu^2}{e}\text{Re}[c^{h_3}_{(22)R}],$$
$$\text{Br}(e_b \to e_a\gamma)[h_3] = \frac{48\pi^2}{G_F^2}(|c^{h_3}_{(ab)R}|^2 + |c^{h_3}_{(ba)R}|^2)\text{Br}(e_b \to e_a\overline{\nu_a}\nu_b). \quad (45)$$

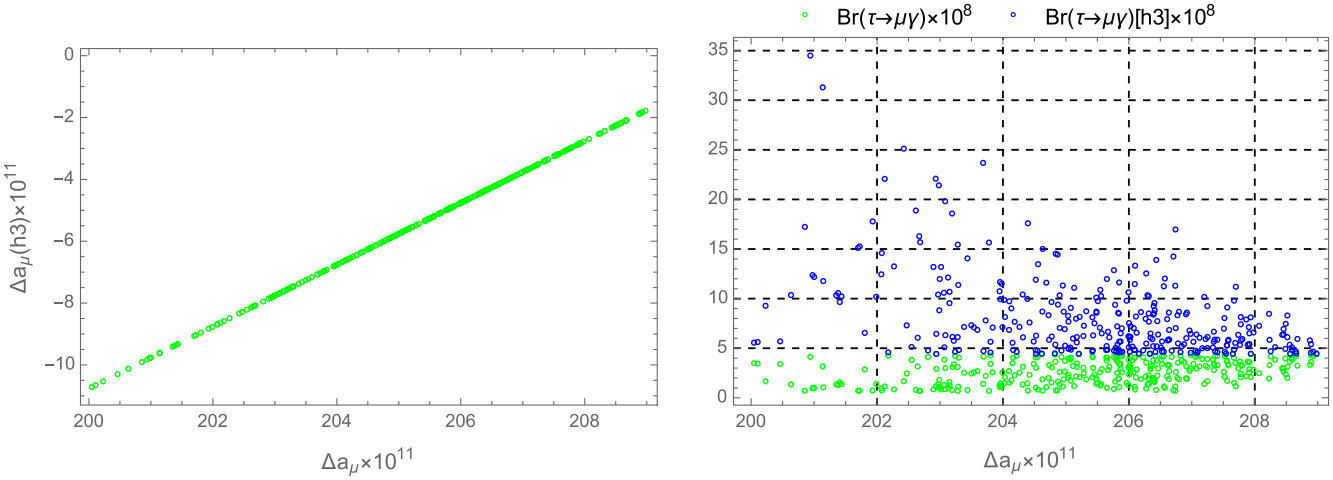

FIG. 2. Correlations between $\Delta a_\mu \equiv \Delta a_\mu^{331\text{ISS}}$ with $\Delta a_\mu(h_3)$ and $\text{Br}(\tau \to \mu\gamma)[h_3]$.

TABLE V. Particular contributions $c^X_{(ab)R}[\mathrm{GeV}^{-2}]$ to Δa_μ and $\mathrm{Br}(e_b \to e_a\gamma)$ with the free parameters shown in Eq. (46). The last column shows values of Δa_μ and $\mathrm{Br}(e_b \to e_a\gamma)$.

Notations	$c^W_{(ab)R} - c^{W,\mathrm{SM}}_{(ab)R}$	$c^Y_{(ab)R}$	$c^{H_1}_{(ab)R}$	$c^{H_2}_{(ab)R}$	$c^{h_3}_{(ab)R}$	$c_{(ab)R}$	Process
$\Delta a_\mu : c_{(22)R} \times 10^{10}$	5.3	−0.386	−211.	61.1	3.7	−141.1	$\Delta a_\mu = 20.5 \times 10^{-10}$
$\mu \to e\gamma : c_{(12)R} \times 10^{13}$	449.16	61.536	−75957.	75443.	0	−2.5234	$\mathrm{Br}(12R) = 2.2174 \times 10^{-13}$
$\mu \to e\gamma : c_{(21)R} \times 10^{13}$	2.1388	0.29303	−361.70	357.43	0	−1.8329	$\mathrm{Br}(21R) = 1.1699 \times 10^{-13}$
$\tau \to e\gamma : c_{(13)R} \times 10^{10}$	−0.00510	0.0540	4.25	−2.96	0	1.34	$\mathrm{Br}(13R) = 111. \times 10^{-10}$
$\tau \to e\gamma : c_{(31)R} \times 10^{10}$	∼0	∼0	0.00120	0.0664	0	0.0676	$\mathrm{Br}(31R) = 0.284 \times 10^{-10}$
$\tau \to \mu\gamma : c_{(23)R} \times 10^{10}$	−0.00721	−0.0445	1.20	−2.51	0.164	−1.20	$\mathrm{Br}(23R) = 86.7 \times 10^{-10}$
$\tau \to \mu\gamma : c_{(32)R} \times 10^{10}$	−0.000426	−0.00263	0.0708	−5.18	2.77	−2.33	$\mathrm{Br}(32R) = 330. \times 10^{-10}$

The corresponding benchmark is calculated numerically with 30 digits of precision number. The numerical values of the free parameters are

$$\begin{aligned} &k_{11} \simeq -19.19, \quad k_{22} \simeq -94.53, \quad k_{33} \simeq 428.75, \quad k_{12} \simeq -89.46, \\ &k_{13} \simeq 29.47, \quad k_{23} \simeq -211.84, \quad k_{21} \simeq 60.09, \quad k_{31} \simeq -262.44, \quad k_{32} \simeq 30.53, \\ &t_\beta = 49.86, \quad z = 1169\ \mathrm{GeV}, \quad m_{H_1} = 657.1\ \mathrm{GeV}, \quad m_{H_2} = 734\ \mathrm{GeV}. \end{aligned} \tag{46}$$

In this case, the heavy neutrino masses are $m_{n_4} = m_{n_5} = 137.2$ GeV, $m_{n_6} = m_{n_7} = 4709.4$ GeV, $m_{n_8} = m_{n_9} = 11958$ GeV. For simplicity we assume that $Y^3_{11} = Y^3_{12} = Y^3_{21} = Y^3_{13} = Y^3_{31} = 0$, therefore the contribution from h_3 does not change the two cLFV decays $\mathrm{Br}(\mu \to e\gamma) \simeq 3.93 \times 10^{-13}$ and $\mathrm{Br}(\tau \to e\gamma) \simeq 1.11 \times 10^{-8}$. They always satisfy the experimental data. The non-zero Yukawa couplings are scanned in the ranges $Y^3_{ab} \in [-3.5, 3.5]$ that satisfy the perturbative limit. This results in the following allowed range of the charged Higgs boson mass 500 GeV $\le m_{h_3} \le$ 1158 GeV. Numerical values of $c_{(ab)R}$ is shown in Table V.

The numerical results shown in Fig. 2 have some interesting properties. In the left panel, the contributions from $h_3^\pm$ to Δa_μ are always negative, but much smaller than the total one: $0 < -\Delta a_\mu(h_3^\pm) \le 1.5 \times 10^{-10} \ll 200 \times 10^{-11} \sim \Delta a_\mu$. On the other hand, the one-loop contributions $c^{h_3}_{(32)R}$ and $c^{H_2}_{(32)R}$ have the same order, but opposite signs. Therefore, the total $|c_{(32)R}|$ is small enough to guarantee that $\mathrm{Br}(\tau \to \mu\gamma) < 4.4 \times 10^{-8}$. This is reason why in the right panel, we see that $|c_{(32)R}| < |c^{h_3}_{(32)R}|$, i.e., $\mathrm{Br}(\tau \to \mu\gamma) < \mathrm{Br}(\tau \to \mu\gamma)[h_3]$ may happen. More specifically, this property can be seen from a particular numerical illustration presented in Table V. We can see a property that $|c_{(22)R}| \gg |c^{h_3}_{(22)R}| \sim |c^{h_3}_{(32)R}| \sim |c^{H_2}_{(32)R}| \sim |c_{(32)R}|$, which explains why the contributions from h_3 affect strongly $\mathrm{Br}(\tau \to \mu\gamma)$ but weakly Δa_μ.

The allowed regions of parameters allowing $\Delta a_\mu^{331\mathrm{ISS}}$ around the value 200×10^{-11} can be found easily in the ranges given in Eq. (44). The allowed regions with larger $\Delta a_\mu^{331\mathrm{ISS}}$ are shown in Fig. 3, where charged Higgs masses have to be smaller than 600 GeV. It is noted that large $\Delta a_\mu^{331\mathrm{ISS}} > 300 \times 10^{-11}$ require light charged Higgs boson masses $m_{H_1} \to 500$ GeV, $z \to 1223$ GeV, and large $t_\beta \to 60$. The region of parameter space corresponding to the Fig 3 is:

$$\begin{aligned} &k_{11} \in [-21.77, -17.84], \quad k_{22} \in [-101.9, -93.76], \quad k_{33} \in [420.1, 429.4], \\ &k_{12} \in [-96.22, -88.92], \quad k_{13} \in [26.95, 31.12], \quad k_{23} \in [-220.2, -210.4], \\ &k_{21} \in [59.19, 66.55], \quad k_{31} \in [-268.6, -262.9], \quad k_{32} \in [25.35, 33.64], \\ &t_\beta \in [41.68, 59.97], \quad z \in [1051, 1223]\ \mathrm{GeV}, \quad m_{H_1} \in [500.6, 631.3]\ \mathrm{GeV}, \\ &m_{H_2} \in [571.3, 703.8]\ \mathrm{GeV}, \quad m_{h_3} \in [500.5, 778.6]\ \mathrm{GeV}, \quad |Y_{22}| \in [0.11, 3.49], \\ &|Y_{23}| \in [0.51, 3.5], \quad |Y_{32}| \in [0.06, 3.49], \quad |Y_{33}| \in [0.009, 3.5]. \end{aligned} \tag{47}$$

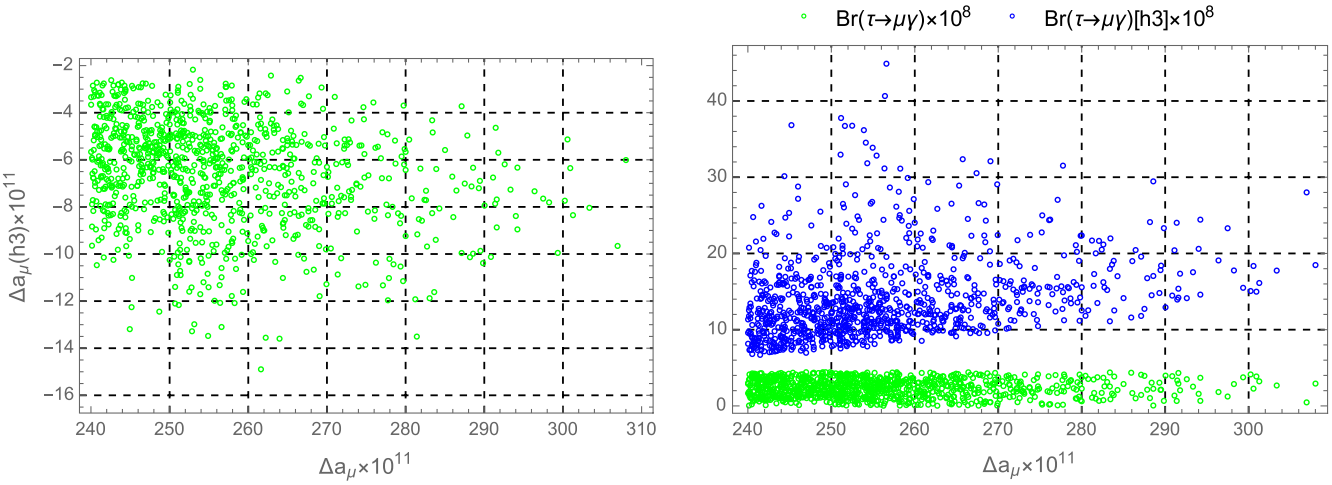

FIG. 3. Correlations between $\Delta a_\mu \equiv \Delta a_\mu^{331\mathrm{ISS}} \geq 240 \times 10^{-11}$ with $\Delta a_\mu(h_3)$ and $\mathrm{Br}(\tau \to \mu\gamma)[h_3]$.

The heavy neutrino masses are in the following ranges: $m_{n_4} = m_{n_5} \in [109.2, 172.3]$ GeV, $m_{n_6} = m_{n_7} \in [3.66, 5.87]$ TeV, $m_{n_8} = m_{n_9} \in [8.99, 14.92]$ TeV. The cLFV branching ratios are in the following ranges: $\mathrm{Br}(\mu \to e\gamma) \times 10^{13} \in [5.8 \times 10^{-16}, 4.2 \times 10^{-13}]$, $\mathrm{Br}(\tau \to e\gamma) \in [4 \times 10^{-11}, 3.3 \times 10^{-8}]$, and $\mathrm{Br}(\tau \to \mu\gamma) \in [1.6 \times 10^{-12}, 4.4 \times 10^{-8}]$.

VI. CONCLUSION

In this work, we have pointed out that the one of the versions of the 3-3-1RN model, namely the 331ISS model, can predict large values of $\Delta a_\mu \simeq 108 \times 10^{-11}$ under the recent constraint of all cLFV decays $e_b \to e_a\gamma$. This large value corresponds to the upper bound $\mathrm{Br}(\tau \to \mu\gamma) \simeq 4.4 \times 10^{-8}$, while the two remaining decay branching ratios are still well below the recent experimental constraints. This model predicts the existence of the two charged Higgs bosons which can give large contributions of the order $\mathcal{O}(10^{-9}) - \mathcal{O}(10^{-8})$ to the Δa_μ, so that it can reach the maximal values around 10^{-9}, which is still much smaller than the allowed values given by the recent experimental data. On the other hand, the two other charged Higgs bosons contributions to $\mathrm{Br}(e_b \to e_a\gamma)$ will be at the orders of $\mathcal{O}(10^{-10}) - \mathcal{O}(10^{-9})[\mathrm{GeV}^{-2}]$. But the huge destructive correlations can happen between these contributions, leading to a small values of $\mathrm{Br}(e_b \to e_a\gamma)$. Although the model contains many free parameters, maybe the antisymmetry of the Dirac mass matrix m_D does not allow large destruction enough to keep the $\mathrm{Br}(\tau \to \mu\gamma)$ below the experimental constraint, while allow large $\Delta a_\mu^{331\mathrm{ISS}} \geq 192 \times 10^{-11}$. The model needs to include an additional singly charged Higgs boson so that all experimental data of Δa_μ and the cLFV decays can be explained simultaneously. As a consequence, all of the cLFV decays $e_b \to e_a\gamma$ are predicted that their branching ratios can be large closely the recent experimental bounds. Therefore, our model can also explain simultaneously all cLFV decays $e_b \to e_a\gamma$ once they are observed by upcoming experiments.

ACKNOWLEDGMENTS

We are grateful to Prof. Martin Hoferichter for introducing us the latest result of the SM prediction of Δa_μ. We thank Prof. Hidezumi Terazawa, Dr. Wen Yin, and Dr. Pengxuan Zhu for their useful information. We would like to express our sincere gratitude to the referee for correcting the electron mass in the original draft, leading to the new numerical illustration in the new version. This research is funded by Vietnam National Foundation for Science and Technology Development (NAFOSTED) under Grant No. 103.01-2018.331.

[1] K. Hagiwara, R. Liao, A. D. Martin, D. Nomura, and T. Teubner, J. Phys. G **38**, 085003 (2011).
[2] M. Davier, A. Hoecker, B. Malaescu, and Z. Zhang, Eur. Phys. J. C **77**, 827 (2017).
[3] R. H. Parker, C. Yu, W. Zhong, B. Estey, and H. Mller, Science **360**, 191 (2018).
[4] P. A. Zyla *et al.* (Particle Data Group), Prog. Theor. Exp. Phys. (**2020**), 083C01.
[5] A. Keshavarzi, D. Nomura, and T. Teubner, Phys. Rev. D **97**, 114025 (2018).
[6] G. Colangelo, M. Hoferichter, and P. Stoffer, J. High Energy Phys. 02 (2019) 006.

[7] M. Hoferichter, B. L. Hoid, and B. Kubis, J. High Energy Phys. 08 (2019) 137.
[8] M. Davier, A. Hoecker, B. Malaescu, and Z. Zhang, Eur. Phys. J. C **80**, 241 (2020); **80**, 410(E) (2020).
[9] A. Keshavarzi, D. Nomura, and T. Teubner, Phys. Rev. D **101**, 014029 (2020).
[10] A. Kurz, T. Liu, P. Marquard, and M. Steinhauser, Phys. Lett. B **734**, 144 (2014).
[11] K. Melnikov and A. Vainshtein, Phys. Rev. D **70**, 113006 (2004).
[12] P. Masjuan and P. Sanchez-Puertas, Phys. Rev. D **95**, 054026 (2017).
[13] G. Colangelo, M. Hoferichter, M. Procura, and P. Stoffer, J. High Energy Phys. 04 (2017) 161.
[14] M. Hoferichter, B. L. Hoid, B. Kubis, S. Leupold, and S. P. Schneider, J. High Energy Phys. 10 (2018) 141.
[15] A. Gérardin, H. B. Meyer, and A. Nyffeler, Phys. Rev. D **100**, 034520 (2019).
[16] J. Bijnens, N. Hermansson-Truedsson, and A. Rodríguez-Sánchez, Phys. Lett. B **798**, 134994 (2019).
[17] G. Colangelo, F. Hagelstein, M. Hoferichter, L. Laub, and P. Stoffer, J. High Energy Phys. 03 (2020) 101.
[18] G. Colangelo, M. Hoferichter, A. Nyffeler, M. Passera, and P. Stoffer, Phys. Lett. B **735**, 90 (2014).
[19] T. Blum, N. Christ, M. Hayakawa, T. Izubuchi, L. Jin, C. Jung, and C. Lehner, Phys. Rev. Lett. **124**, 132002 (2020).
[20] T. Aoyama, M. Hayakawa, T. Kinoshita, and M. Nio, Phys. Rev. Lett. **109**, 111808 (2012).
[21] T. Aoyama, T. Kinoshita, and M. Nio, Atoms **7**, 28 (2019).
[22] A. Czarnecki, W. J. Marciano, and A. Vainshtein, Phys. Rev. D **67**, 073006 (2003); **73**, 119901(E) (2006).
[23] C. Gnendiger, D. Stöckinger, and H. Stöckinger-Kim, Phys. Rev. D **88**, 053005 (2013).
[24] T. Aoyama, N. Asmussen, M. Benayoun, J. Bijnens, T. Blum, M. Bruno, I. Caprini, C. M. Carloni Calame, M. Cè, G. Colangelo *et al.*, Phys. Rep. **887**, 1 (2020).
[25] B. Abi *et al.* (Muon g-2 Collaboration), Phys. Rev. Lett. **126**, 141801 (2021).
[26] B. Aubert *et al.* (*BABAR* Collaboration), Phys. Rev. Lett. **104**, 021802 (2010).
[27] A. M. Baldini *et al.* (MEG Collaboration), Eur. Phys. J. C **76**, 434 (2016).
[28] N. A. Ky, H. N. Long, and D. V. Soa, Phys. Lett. B **486**, 140 (2000).
[29] C. Kelso, H. N. Long, R. Martinez, and F. S. Queiroz, Phys. Rev. D **90**, 113011 (2014).
[30] D. T. Binh, D. T. Huong, L. T. Hue, and H. N. Long, Commun. Phys. **25**, 29 (2015).
[31] A. S. De Jesus, S. Kovalenko, F. S. Queiroz, C. Siqueira, and K. Sinha, Phys. Rev. D **102**, 035004 (2020).
[32] Á. S. de Jesus, S. Kovalenko, C. A. de S. Pires, F. S. Queiroz, and Y. S. Villamizar, Phys. Lett. B **809**, 135689 (2020).
[33] M. Lindner, M. Platscher, and F. S. Queiroz, Phys. Rep. **731**, 1 (2018).
[34] A. E. Cárcamo Hernández, D. T. Huong, and H. N. Long, Phys. Rev. D **102**, 055002 (2020).
[35] A. E. Cárcamo Hernández, Y. Hidalgo Velásquez, S. Kovalenko, H. N. Long, N. A. Pérez-Julve, and V. V. Vien, Eur. Phys. J. C **81**, 191 (2021).
[36] L. T. Hue, N. T. Phong, and T. D. Tham, Commun. Phys. **30**, 221 (2020).
[37] B. Snchez-Vega, E. Schmitz, and J. Montero, Eur. Phys. J. C **78**, 166 (2018).
[38] D. Chang and H. N. Long, Phys. Rev. D **73**, 053006 (2006).
[39] M. E. Catano, R. Martinez, and F. Ochoa, Phys. Rev. D **86**, 073015 (2012).
[40] A. G. Dias, C. A. de S.Pires, P. S. Rodrigues da Silva, and A. Sampieri, Phys. Rev. D **86**, 035007 (2012).
[41] S. M. Boucenna, J. W. F. Valle, and A. Vicente, Phys. Rev. D **92**, 053001 (2015).
[42] C. A. de Sousa Pires, F. F. De Freitas, J. Shu, L. Huang, and P. W. V. Olegrio, Phys. Lett. B **797**, 134827 (2019).
[43] A. M. Baldini, F. Cei, C. Cerri, S. Dussoni, L. Galli, M. Grassi, D. Nicolo, F. Raffaelli, F. Sergiampietri, G. Signorelli *et al.*, arXiv:1301.7225.
[44] T. Aushev, W. Bartel, A. Bondar, J. Brodzicka, T. E. Browder, P. Chang, Y. Chao, K. F. Chen, J. Dalseno, A. Drutskoy *et al.*, arXiv:1002.5012.
[45] J. Cao, J. Lian, L. Meng, Y. Yue, and P. Zhu, Phys. Rev. D **101**, 095009 (2020).
[46] J. Cao, Y. He, J. Lian, D. Zhang, and P. Zhu, arXiv:2102.11355.
[47] T. Nomura, H. Okada, and P. Sanyal, arXiv:2103.09494.
[48] T. Mondal and H. Okada, arXiv:2103.13149.
[49] T. P. Nguyen, T. T. Le, T. T. Hong, and L. T. Hue, Phys. Rev. D **97**, 073003 (2018).
[50] R. Foot, H. N. Long, and T. A. Tran, Phys. Rev. D **50**, R34 (1994).
[51] A. J. Buras, F. De Fazio, J. Girrbach, and M. V. Carlucci, J. High Energy Phys. 02 (2013) 023.
[52] A. J. Buras, F. De Fazio, and J. Girrbach-Noe, J. High Energy Phys. 08 (2014) 039.
[53] L. Hue and L. Ninh, Eur. Phys. J. C **79**, 221 (2019).
[54] L. T. Hue, H. N. Long, T. T. Thuc, and T. P. Nguyen, Nucl. Phys. **B907**, 37 (2016).
[55] A. E. Cárcamo Hernández, S. Kovalenko, H. N. Long, and I. Schmidt, J. High Energy Phys. 07 (2018) 144.
[56] M. Tanabashi *et al.* (Particle Data Group), Phys. Rev. D **98**, 030001 (2018).
[57] K. Abe *et al.* (T2K Collaboration), Nature (London) **580**, 339 (2020); **583**, E16 (2020).
[58] W. Yin, arXiv:2103.14234.
[59] M. J. Baker, P. Cox, and R. R. Volkas, J. High Energy Phys. 05 (2021) 174.
[60] L. D. Ninh and H. N. Long, Phys. Rev. D **72**, 075004 (2005).
[61] L. T. Hue, L. D. Ninh, T. T. Thuc, and N. Dat, Eur. Phys. J. C **78**, 128 (2018).
[62] A. Crivellin, M. Hoferichter, and P. Schmidt-Wellenburg, Phys. Rev. D **98**, 113002 (2018).
[63] G. W. Bennett *et al.* (Muon (g-2) Collaboration), Phys. Rev. D **80**, 052008 (2009).
[64] F. Jegerlehner and A. Nyffeler, Phys. Rep. **477**, 1 (2009).
[65] T. Aoyama, M. Hayakawa, T. Kinoshita, and M. Nio, Phys. Rev. Lett. **109**, 111807 (2012).
[66] S. Laporta, Phys. Lett. B **772**, 232 (2017).
[67] H. Terazawa, Nonlin. Phenom. Complex Syst. **21**, 268 (2018).
[68] S. Volkov, Phys. Rev. D **100**, 096004 (2019).